

CXCR4/CXCL12 Mediate Autocrine Cell-Cycle Progression in NF1-Associated Malignant Peripheral Nerve Sheath Tumors

Wei Mo,¹ Jian Chen,¹ Amish Patel,² Liang Zhang,³ Vincent Chau,^{1,2} Yanjiao Li,¹ Woosung Cho,¹ Kyun Lim,¹ Jing Xu,¹ Alexander J. Lazar,⁴ Chad J. Creighton,⁶ Svetlana Bolshakov,⁵ Renée M. McKay,¹ Dina Lev,⁵ Lu Q. Le,^{2,*} and Luis F. Parada^{1,*}

¹Department of Developmental Biology

²Department of Dermatology

³Department of Cell Biology

University of Texas Southwestern Medical Center, Dallas, TX 75390-9133, USA

⁴Department of Pathology

⁵Department of Cancer Biology

University of Texas MD Anderson Cancer Center, Houston, TX 77054, USA

⁶Division of Biostatistics, Dan L. Duncan Cancer Center, Baylor College of Medicine, Houston, TX 77030, USA

*Correspondence: lu.le@utsouthwestern.edu (L.Q.L.), luis.parada@utsouthwestern.edu (L.F.P.)

<http://dx.doi.org/10.1016/j.cell.2013.01.053>

SUMMARY

Malignant peripheral nerve sheath tumors (MPNSTs) are soft tissue sarcomas that arise in connective tissue surrounding peripheral nerves. They occur sporadically in a subset of patients with neurofibromatosis type 1 (NF1). MPNSTs are highly aggressive, therapeutically resistant, and typically fatal. Using comparative transcriptome analysis, we identified CXCR4, a G-protein-coupled receptor, as highly expressed in mouse models of NF1-deficient MPNSTs, but not in nontransformed precursor cells. The chemokine receptor CXCR4 and its ligand, CXCL12, promote MPNST growth by stimulating cyclin D1 expression and cell-cycle progression through PI3-kinase (PI3K) and β -catenin signaling. Suppression of CXCR4 activity either by shRNA or pharmacological inhibition decreases MPNST cell growth in culture and inhibits tumorigenesis in allografts and in spontaneous genetic mouse models of MPNST. We further demonstrate conservation of these activated molecular pathways in human MPNSTs. Our findings indicate a role for CXCR4 in NF1-associated MPNST development and identify a therapeutic target.

INTRODUCTION

The tumor predisposition disorder von Recklinghausen's neurofibromatosis type I (NF1) is one of the most common genetic disorders of the nervous system, affecting one in 3,500 individuals worldwide (Zhu and Parada, 2001). A cardinal feature of NF1 is the growth of benign tumors called neurofibromas, categorized into plexiform and dermal subtypes (Le and Parada, 2007). Plexiform neurofibromas can undergo malignant transfor-

mation into neurofibrosarcomas, known as malignant peripheral nerve sheath tumors (MPNSTs), which represent a major source of morbidity for NF1 patients (Ferner, 2007). Despite continued progress in understanding NF1 biology, MPNST treatment remains limited to surgery, and prognosis remains unchanged (Tongsgard, 2006).

The development of murine models has provided an opportunity to gain insight into NF1-deficient tumor natural history (Cichowski et al., 1999; Joseph et al., 2008; Vogel et al., 1999; Zheng et al., 2008; Zhu et al., 2002). *NF1* and *TP53*, or *CDKN2a*, are the most frequently mutated cancer-related genes in human MPNSTs (Mantripragada et al., 2008; Rubin and Gutmann, 2005). Our genetically engineered mouse models (GEMMs) recapitulate tumors that arise in NF1 patients, and we and others have shown that genetic ablation of the *NF1* and *p53* tumor suppressors results in spontaneous development of MPNSTs (Cichowski et al., 1999; Vogel et al., 1999). Benign and malignant *Nf1*-deficient tumors can also be induced by subcutaneous implantation of *Nf1*- or *Nf1;p53*-deficient skin-derived precursor (SKPs), respectively, and are histologically indistinguishable from human counterparts (Le et al., 2009); L.Q.L., T. Shipman, and L.F.P., unpublished data).

Here, we examine the chemokine receptor CXCR4, which we find enriched in *Nf1*-deficient cells and particularly in *Nf1*-deficient MPNSTs. Expression of CXCR4 and its ligand, CXCL12, has been reported in solid tumors, (Kijima et al., 2002; Koshiba et al., 2000; Laverdiere et al., 2005; Müller et al., 2001; Oh et al., 2001; Righi et al., 2011; Schrader et al., 2002; Sehgal et al., 1998; Sengupta et al., 2012; Taichman et al., 2002; Zeelenberg et al., 2003; Zhou et al., 2002) as well as non-Hodgkin's lymphoma (Bertolini et al., 2002) and chronic lymphocytic leukemia (Burger et al., 1999). Clinical data indicate that high CXCR4 correlates with poor clinical outcome (Bian et al., 2007; Li et al., 2004; Wang et al., 2008). The proposed paracrine roles for CXCR4/CXCL12 in a variety of tumorigenic processes include cell growth (Schrader et al., 2002; Zhou et al., 2002),

metastasis (Li et al., 2004), and angiogenesis (Sengupta et al., 2012).

A potential role for CXCR4 in sarcoma pathogenesis has not been examined. Here, we provide evidence that the CXCR4/CXCL12 axis is essential for MPNST tumor progression. Specifically, the autocrine activation of CXCR4 by CXCL12 triggers intracellular PI3-kinase (PI3K) and β -catenin signals to promote G1 to S phase transition in MPNST cells. The CXCR4 antagonist, AMD3100, has growth-inhibitory effects on primary cultured mouse and human MPNST cells, tumor allografts, and spontaneous GEMMs. Moreover, analysis of human primary and cultured MPNST cells, as well as human tissue microarray analysis, reveals conserved pathway activation. Thus, CXCR4 inhibition may represent a therapeutic strategy to treat MPNST.

RESULTS

CXCR4 in *Nf1*-Deficient MPNST Tumors

Previously, we demonstrated that *Nf1*-deficient SKPs can give rise to either dermal or plexiform neurofibromas depending on their local microenvironment (dermis versus sciatic nerve) (Le et al., 2009). In addition, dual mutation of the *Nf1* and *p53* tumor suppressors in these cells results in MPNSTs that exhibit cellular and molecular features of human MPNSTs (L.Q.L., T. Shipman, and L.F.P., unpublished data). These tumors are indistinguishable from a spontaneous MPNST GEMM also based on loss of *Nf1* and *p53* (*cisNP*; Cichowski et al., 1999; Vogel et al., 1999). To gain insight into the molecular and cellular mechanisms underlying development of *Nf1*-deficient MPNSTs, we used microarray analysis to compare the transcriptomes of MPNSTs with those of normal SKPs (WT), as well as pretumorigenic SKPs with either *Nf1* deletion (*Nf1*^{-/-}) or *Nf1* and *p53* (*NP*^{-/-}) deletion, as shown in Figure 1A. The comparative array data presented a complex picture of up- and downregulated transcripts for diverse genes (data not shown). However, our attention was drawn to the elevated expression of the chemokine receptor CXCR4 that exhibited a 3-fold elevation in both pretumor cell types (*Nf1*^{-/-}; *NP*^{-/-}) and a 12-fold increase in the malignant form of SKP MPNST (SMPNST). Quantitative RT-PCR and western blot analysis (Figures 1B and 1C) confirmed these array data. We also measured low CXCR4 levels in Schwann cells, which belong to the embryonic lineage of origin of *Nf1*-deficient tumors (Le et al., 2011; Serra et al., 2000; Zhu et al., 2002), and high levels in tumor cells from the spontaneous *cisNP* mouse model of MPNST by western blot (Figure S1A available online; [Vogel et al., 1999]) and immunohistochemistry (IHC). We further performed IHC on tumor samples from the SMPNST-allograft, *cisNP*, and SMPNST-autograft models and a human MPNST sample (Figures 1D and S1B). Together, these data confirmed elevated CXCR4 protein in the different sources of *Nf1*-deficient malignant tissues compared to controls and, further, provided evidence that CXCR4 expression is sustained in human *NF1*-associated MPNST.

CXCR4 Knockdown Impairs Cell Proliferation and Attenuates Tumorigenesis

To evaluate the functional role of CXCR4 in MPNST pathogenesis, we used short hairpin RNA (shRNA) for knockdown in

SMPNST cells. Cells were infected with lentivirus containing CXCR4 shRNA or a control scrambled shRNA (pLKO ctrl), and stable cell lines were established using puromycin selection. Two different shRNA sequences, targeting either the coding region (pLKO-mCXCR4) or the 3' UTR (pLKO-mCXCR4-UTR) reduced CXCR4 messenger RNA (mRNA) levels by ~90% (Figures S2A and S2B). To address whether CXCR4 influences SMPNST cell metabolism, we measured ATP levels using a luminescence assay and found that tumor cells with depleted CXCR4 were less metabolically active. Introduction of exogenous CXCR4 complementary DNA (cDNA) lacking the UTR sequences (so that it is not targeted by the shRNA) re-established CXCR4 protein levels and overcame the cell growth inhibition (Figures 2A and S2B).

We turned to a doxycycline (dox)-inducible Mir30-based shRNA system to enable acute knockdown of CXCR4. Using this system, murine and human CXCR4 mRNA levels were decreased to 25% and 10% of the origin level, respectively (Figures S2C–S2F). In contrast, induction with dox had no effect on CXCR4 expression in MPNST-Tripz-scrambled control cells (Figures S2C–S2F). Similar to the pLKO knockdown results, we observed cell growth arrest in CXCR4-depleted SMPNST and human MPNST (S462) cells upon dox treatment (Figure 2B). Together, these results confirm that CXCR4 plays a role in murine- and human-derived MPNST cell proliferation.

We next investigated the growth properties of tumor cells in vivo after CXCR4 knockdown. 10⁴ or 10⁵ pLKO-mCXCR4 or pLKO-ctrl SMPNST cells were injected subcutaneously into nude mice and monitored for tumor growth (SMPNST-allografts). The mice were sacrificed and tumors were dissected 1 month after injection (Figure S2G). Quantification of tumor size and weight showed that MPNST cells with CXCR4 knockdown generated smaller tumors than control cells (Figure S2H), and additionally, time to tumor appearance was significantly increased (Figure S2I). We also analyzed cell proliferation in excised tumors and found the average percentage of Ki67-positive, proliferating cells was 24.2% \pm 6.5% in CXCR4-depleted MPNSTs versus 67.6% \pm 5.1% in controls (Figures S2J and S2K).

Similar results were obtained when the inducible shRNA tumor cells were implanted and subjected to dox-mediated CXCR4 knockdown after the tumor cells had successfully seeded in the allograft. This approach eliminated the possibility that CXCR4 knockdown in culture impeded subsequent tumor cell implantation. 10⁴ or 10⁵ MPNST-Tripz-CXCR4 cells were injected subcutaneously into nude mice, and one group received dox (1 mg/ml) in the drinking water (Figure 2C). Compared to controls, tumor appearance in the dox-treated group was delayed by 1 week, and tumor progression was impaired (Figures 2C and 2D). All mice were sacrificed on day 26, and tumors were excised. Western blot analysis showed an ~73.1% depletion of CXCR4 protein in the tumors harvested from dox-treated mice (Figure 2E). When 10⁵ cells were injected, 6/6 control mice bore tumors (759 \pm 500 mm³ in size and 0.467 \pm 0.226 g in weight), and 5/6 dox-treated mice developed tumors that were smaller both in size (199 \pm 115 mm³) and weight (0.1 \pm 0.08 g) (Figures 2F and 2G). Notably, when 10⁴ cells were injected, no dox-treated mice developed tumors, whereas control group

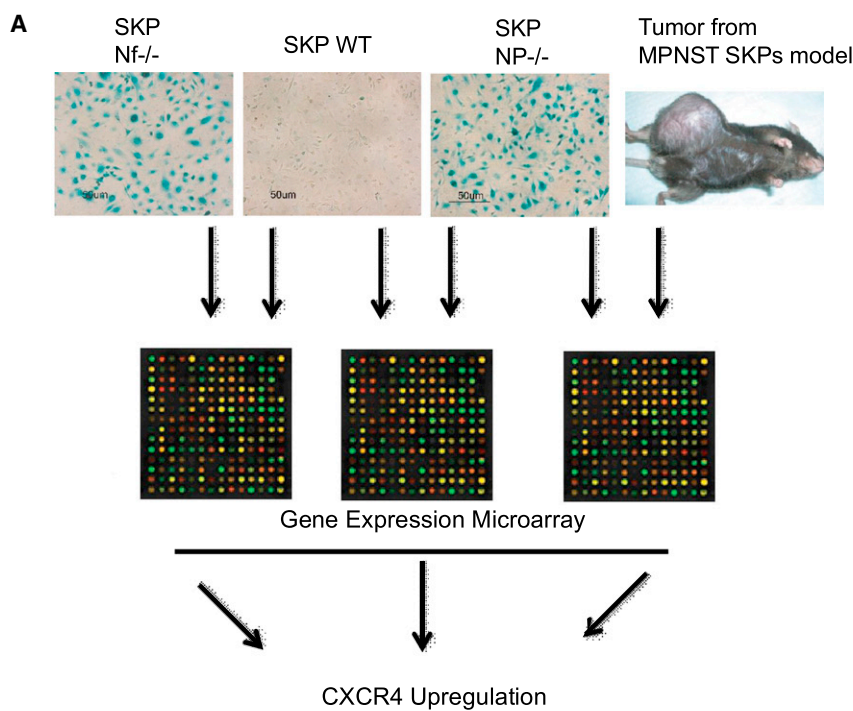
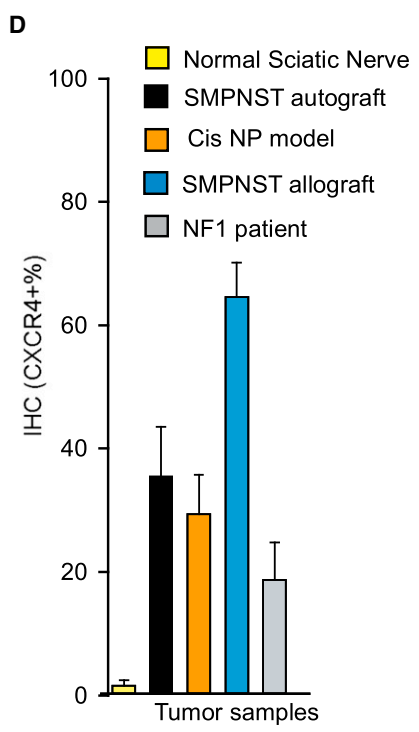
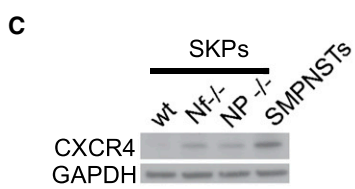
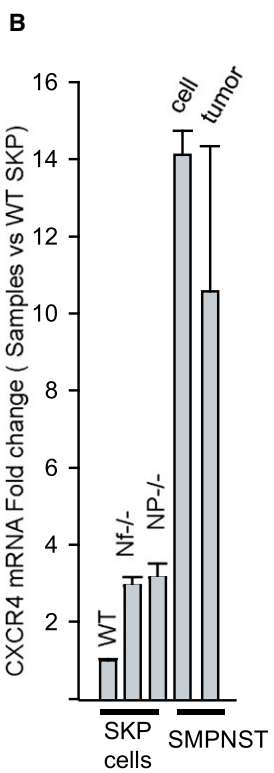


Figure 1. CXCR4 Is Overexpressed in MPNSTs

(A) Schema of the microarray analyses.
 (B) qRT-PCR analysis of CXCR4 mRNA levels in WT, *Nf*^{-/-}, and *NP*^{-/-} (*Nf*^{-/-}; *p53*^{-/-}) SKPs, as well as MPNST SKP model tumors and the cells derived from the tumor.
 (C) Western blot analysis of CXCR4 protein levels in *Nf*^{-/-} and *NP*^{-/-} SKPs and SMPNST cancer cells.
 (D) Quantification of CXCR4-positive cells in tumor tissues from different mouse models of MPNST and an MPNST from an NF1 patient (SMPNST = SMPNST autograft; athymic model = SMPNST allograft).
 All statistics represent mean ±SD. See also Figure S1.



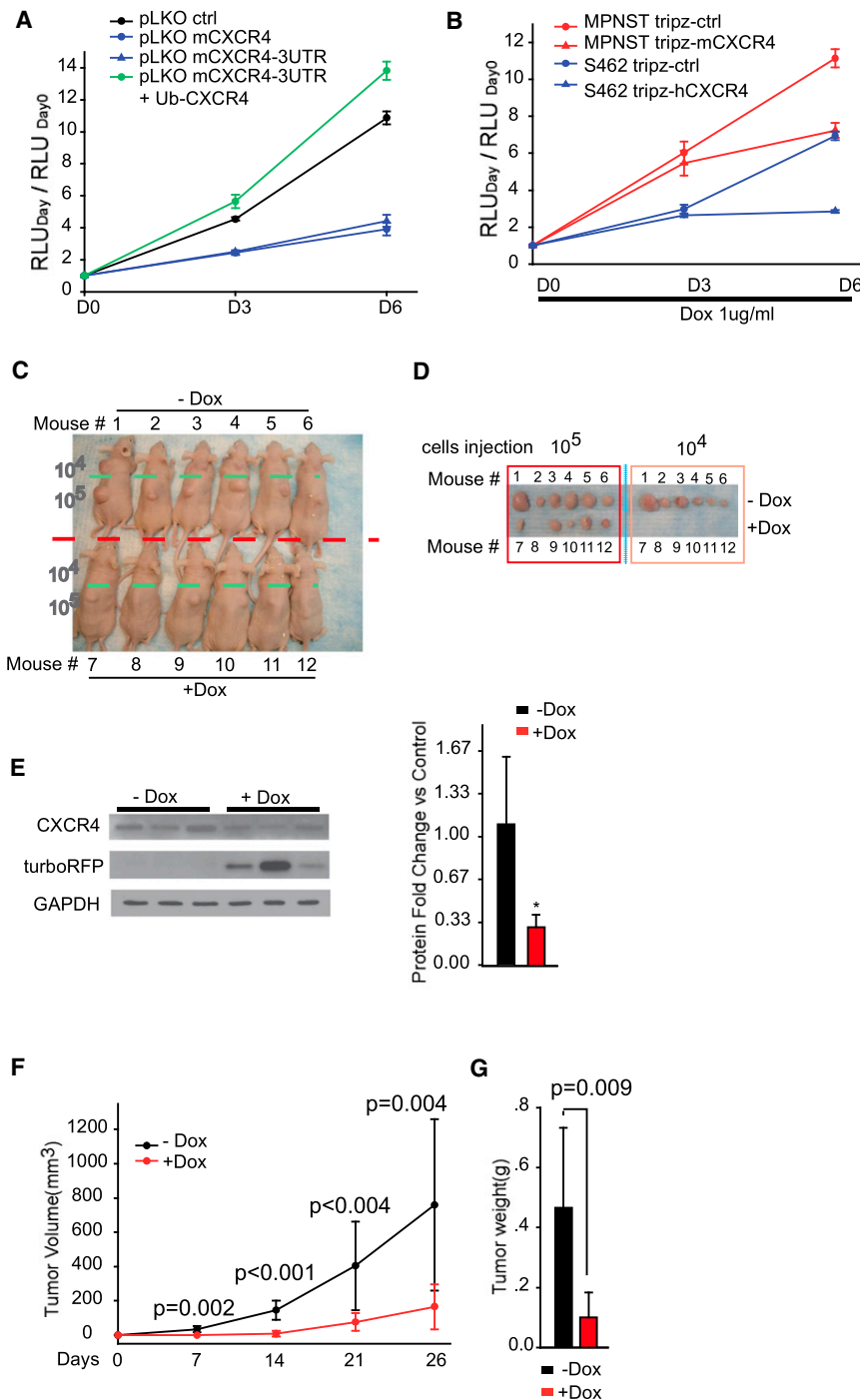


Figure 2. Knockdown of CXCR4 Expression in MPNST Cells Decreased Proliferation In Vitro and Tumorigenesis In Vivo

(A and B) ATP luminescence assays were used to measure growth of indicated cells. (C and D) Representative pictures of the tumors from nude mice injected with SMPNST-Tripz-mCXCR4 cells. Mice 1–6: without Dox treatment; mice 7–12: Dox treatment. (E) CXCR4 protein level is downregulated in dox-treated MPNSTs. (F) Kinetic curve of tumor growth as measured by tumor volume. (G) Quantification of tumor weight. All statistics represent mean \pm SD. See also Figure S2.

S3A and S3B) or senescence (Figures S3C and S3D). Bromodeoxyuridine (BrdU) incorporation and fluorescence-activated cell sorting (FACS) analysis showed significant reduction in BrdU incorporation in CXCR4-depleted cells ($57.2\% \pm 3.6\%$ versus $21.8\% \pm 2.6\%$; Figure 3A). When CXCR4 protein level was restored, the percentage of BrdU-positive cells was also restored to that of CXCR4-WT cells (Figure 3A). Additional cell-cycle analysis revealed that the percentage of cells in G1 phase was $\sim 60\%$ in CXCR4-depleted SMPNST cells versus $\sim 25\%$ in CXCR4-WT cells; by contrast, the number of cells in G2/M phase was only slightly changed (Figures 3B and S3E). These data suggest that CXCR4-depleted MPNST cells undergo G1/S arrest. We also performed BrdU incorporation studies in vivo. Tumor-bearing mice were injected with BrdU 3 hr before sacrifice. BrdU IHC revealed $42\% \pm 11\%$ BrdU-positive cells in the tumor samples from mice injected with control SMPNST cells. In contrast, the BrdU-positive cell number decreased to $15\% \pm 5\%$ in the tumor samples from mice injected with CXCR4-depleted SMPNST cells (Figures 3C and 3D). Similar to the MPNST cell culture results, there was no obvious apoptosis in either tumor group (Figures S3F and S3G). In

mice developed tumors (Figure 2D). Thus, both chronic and acute suppression of CXCR4 in vivo substantially decreased the tumorigenic capacity of MPNST cells.

CXCR4 Depletion Alters the MPNST Cell Cycle

We investigated possible mechanisms of CXCR4 function in promoting MPNST progression. shRNA depletion caused growth arrest of SMPNSTs (Figure 2) rather than apoptosis (Figures

summary, knockdown of CXCR4 expression, in culture and in vivo, led to cell-cycle arrest manifested by reduced S phase and BrdU incorporation, rather than cell death or senescence.

Cyclin D1 Expression Is Regulated by CXCR4

We next investigated whether CXCR4 perturbation impacts the expression of cell-cycle-regulatory genes (Johnson and Walker, 1999; Lee and Yang, 2003; Obaya and Sedivy, 2002). Although

quantitative RT-PCR (qRT-PCR) analysis indicated that expression of most genes examined was unchanged in CXCR4-depleted SMPNST cells and tumors, cyclin D1 mRNA levels decreased ~70% (Figures 3E and S3H). A slight reduction in CDK4/6 and cyclin E mRNA levels was also observed (Figures 3E and S3H). Quantification of western blots confirmed the cyclin D1 protein level decrease in CXCR4-depleted MPNST cells and tumors (SMPNST allografts) (Figures 3F and S3I). Both cyclin D1 mRNA and protein levels were fully restored in CXCR4-depleted MPNST cells with exogenous CXCR4 expression (Figures 3E and 3F). Moreover, reintroduction of cyclin D1 cDNA restored protein levels and counteracted the CXCR4 depletion effect, allowing cells to resume progression through the cell cycle (Figures 3G and 3H). These data demonstrate that, in SMPNST cells, cell-cycle progression mediated by cyclin D1 is dependent on CXCR4 function.

CXCR4 Activates the AKT/GSK-3 β / β -Catenin Network

Signaling pathways known to regulate cyclin D1 include the NF κ B, Ras, ERK, Wnt/ β -catenin, and JAK/STAT3 pathways (Sherr, 1995). To determine whether any of these candidate pathways mediate CXCR4 regulation of cyclin D1 in neurofibrosarcomas, fractionated nuclear and cytoplasmic extracts of SMPNST cells were immunoblotted with the indicated antibodies to examine changes following CXCR4 depletion. We observed that both cyclin D1 and β -catenin levels decreased 76.4% and 77.3%, respectively, in the nuclear fraction of CXCR4-depleted MPNST cells (Figure 4A). No changes were seen in other pathways examined (Figure 4A). Transcriptional activation assays using a luciferase reporter linked to the T cell factor (TCF) promoter—a physiological target of β -catenin—showed a 57% reduction in luciferase activity in CXCR4-depleted SMPNST cells compared to controls, which is consistent with the model that suppression of CXCR4 attenuated β -catenin activity (Figure 4B). To test whether nuclear β -catenin is required for cyclin D1 expression, we directly blocked TCF function (Hoppler and Kavanagh, 2007). Expression of dominant-negative TCF (dnTCF) dramatically decreased cyclin D1 mRNA and protein levels in CXCR4-WT-MPNST cells (Figures 4C and 4D), whereas overexpression of β -catenin in CXCR4-depleted MPNST cells restored cyclin D1 expression (Figure 4E) and, further, rescued the cell growth arrest caused by CXCR4 knockdown (Figure 4F). Functionally, downregulation of the β -catenin pathway by dnTCF resulted in cell growth arrest in MPNST cells (Figure S4A). We also examined tumors for β -catenin expression. IHC on MPNST tumor tissues from SMPNSTs (SMPNST allografts) (Figure S4B) and one human patient sample (Figure S4C) showed robust nuclear immunoreactivity consistent with activation of β -catenin signaling in these tumors.

The above data demonstrate a role for β -catenin downstream of CXCR4 and upstream of TCF and cyclin D1 in stimulating MPNST growth. β -catenin stabilization is required for its role as a transcription factor. In the inactive state, β -catenin is destabilized by phosphorylation at Ser33, Ser37, and Thr41 by GSK-3 β or at Ser45 by CK1 α (Liu et al., 2002). Western blot analysis showed that CXCR4 depletion increased β -catenin serine phosphorylation at sites 33/37, but not 45 (Figure 4G), suggesting that CXCR4 suppression resulted in GSK-3 β kinase activation. We

also examined GSK-3 β serine 9 inactivating phosphorylation and observed a reduction in CXCR4-depleted MPNST cells (Figure 4G). Thus, in MPNST, CXCR4 activity maintains GSK-3 β in the inactive state. GSK-3 β is in turn a downstream element of the PI3K/AKT signaling pathway (Cross et al., 1995) whose kinase activity is inhibited by AKT-mediated phosphorylation at Ser9 (Srivastava and Pandey, 1998). We reasoned that the decreased phosphoSer9-GSK-3 β level in CXCR4-depleted MPNST cells might result from attenuated AKT kinase activity and confirmed this by western blot analysis with pAKT (Ser473) antibody (Figure 4G). We also found reduced levels of activated β -catenin, pGSK-3 β (Ser9), and pAKT (Ser473) in CXCR4-depleted MPNST tumor samples compared to control tumors (SMPNST allografts) (Figure 4H). These data support the model that CXCR4 promotes MPNST growth by activating the PI3K/AKT and the GSK-3 β / β -catenin pathways. Previous *in vitro* studies using human and murine MPNST cell lines, as well as *in vivo* studies using the *cisNP* mouse model, demonstrated that the mTOR pathway can regulate MPNST growth by posttranscriptional regulation of cyclin D1 (Johannessen et al., 2008). We observed modest reduction in phospho-mTOR upon CXCR4 knockdown, but this was not accompanied by obvious change in the levels of phosphorylated-S6 ribosomal protein (Figure S4D). Collectively, our data indicate that CXCR4 regulates the activity of β -catenin via the AKT/GSK-3 β cascade, which ultimately controls cyclin D1 transcription and protein levels.

CXCL12 Activates CXCR4 in an Autocrine Loop

We sequenced CXCR4 cDNAs from two independent murine MPNSTs, one derived from the SMPNST-allograft model and one from the *cisNP* model, and found no missense or nonsense mutations (data not shown). Moreover, CXCR4-activating mutations have not been identified in MPNST cell lines or primary cells derived from human patients (see below and Figure S5A). Therefore, in these tumors, receptor activity must rely on the presence of ligand—CXCL12. qPCR analysis showed that CXCL12 mRNA was indeed elevated in pretumorigenic SKPs (*NP*^{-/-}) and was even more highly expressed in SMPNST tumor cells (Figure S5B). To test the role of CXCL12 in MPNST cell growth, we treated cultured MPNST cells with recombinant CXCL12 protein and found that it promoted cell growth, generating a 1.5-fold increase in cell number at a concentration of 10 ng/ml by day 6, when compared to nontreated cells (Figure 5A). In contrast, cell number decreased by 25% and 55% at days 3 and 6, respectively, when cells were cultured with anti-CXCL12 antibody compared to IgG or PBS control (Figure 5B). These data suggest that CXCL12 is critical for MPNST cell proliferation. To verify the autocrine source of CXCL12 ligand in the MPNST cell culture, we performed an ELISA on the medium conditioned by MPNST cells using an anti-CXCL12 antibody. We observed no detectable CXCL12 protein in control media (with no cells) compared to the conditioned media, indicating that the *in vitro* source of CXCL12 protein is the MPNST cells (Figure 5C). Consistent with the ELISA showing that conditioned media from CXCL12-overexpressing MPNST cells (pBabe-CXCL12) and knockdown cells (pLKO-CXCL12) contained elevated and reduced cytokine, respectively (Figures 5C and S5C), CXCL12-overexpressing

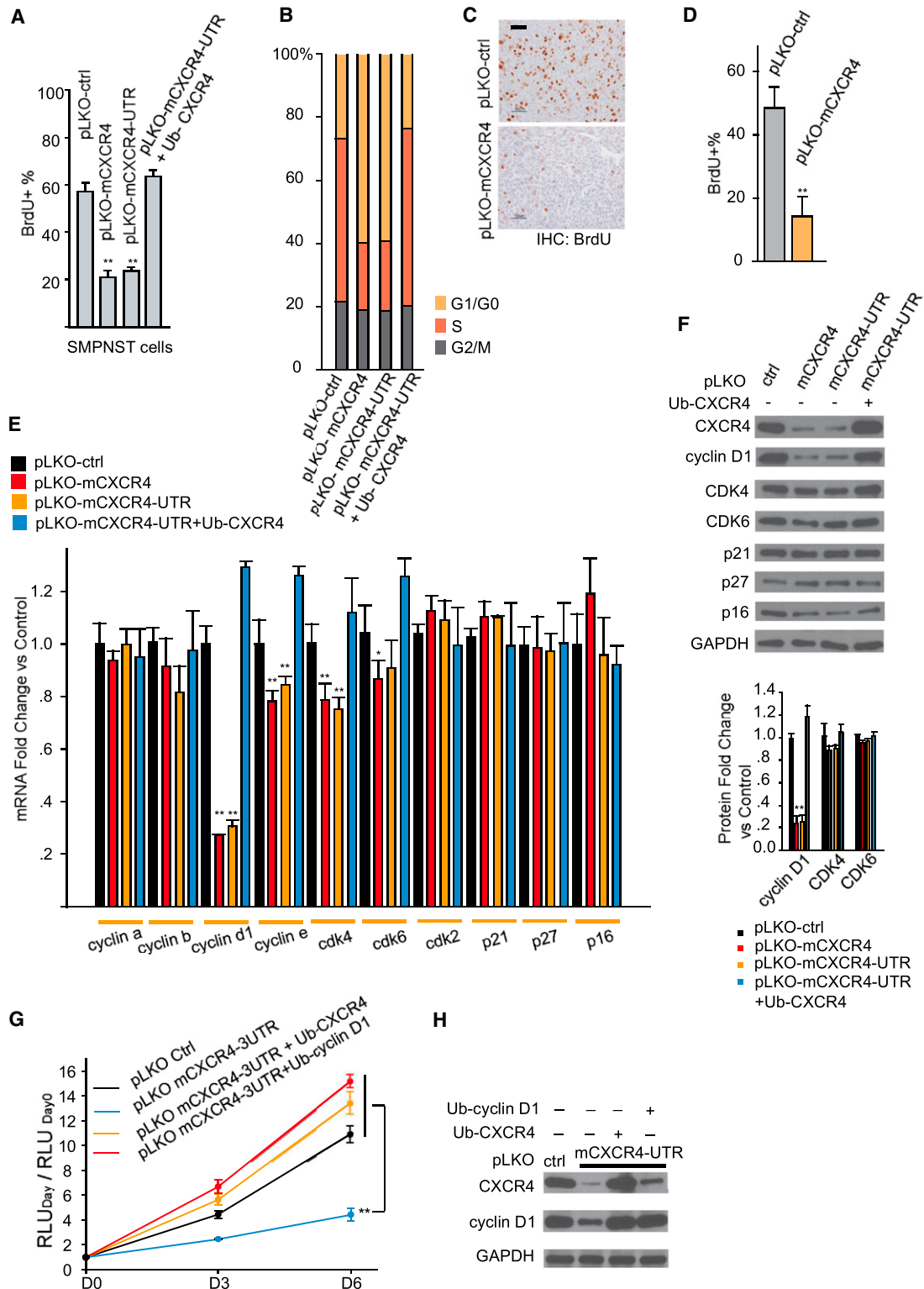


Figure 3. CXCR4 Alters the Cell Cycle in SMPNST Cells by Regulating Cyclin D1 Expression

SMPNST cells were incubated with BrdU for 30 min and then stained with propidium iodide.

(A and B) FACS analysis showed that CXCR4 depletion in SMPNST cells decreased the percentage of BrdU-positive cells (pLKO-mCXCR4 and pLKO-mCXCR4-UTR compared to control pLKO-ctrl) (A) and altered the proportion of cells in G1 and S phases (B). Expression of CXCR4 in the knockdown cells (pLKO-mCXCR4-UTR + Ub-CXCR4) restored the cells to the control state.

(legend continued on next page)

cells had a significant growth advantage (Figure 5A), whereas CXCL12 knockdown cells exhibited a significant reduction in growth at days 3 and 6 (Figure 5D). Importantly, the cell growth inhibition could be rescued by addition of CXCL12 protein (Figure 5E). Therefore, MPNST cells synthesize and secrete CXCL12 protein, causing increased cell growth that corresponded with CXCL12 levels. To confirm that the effect of CXCL12 on MPNST growth is dependent on CXCR4, we added CXCL12 protein to cultured CXCR4-depleted MPNST cells. We found no detectable change in cell proliferation after ligand stimulation compared to control CXCR4-depleted MPNST cells (Figure 5E). Additionally, CXCL12 modulation in the presence of receptor induced the same signaling pathway changes brought about by CXCR4 modulation (Figure 5F). Taken together, these data demonstrate that CXCL12, secreted by MPNST cells, is sufficient to sustain autocrine activation of its receptor, CXCR4, and triggers specific downstream signaling pathways, leading to MPNST cell-cycle progression and proliferation.

Given the important roles of CXCR4/CXCL12 in tumor angiogenesis, we also investigated whether CXCR4 depletion in MPNST cells altered the microvasculature. Both control and CXCR4-depleted tumors exhibit strong CD31 staining (Figure S5D) and similar vessel densities (Figure S5E), indicating that the tumor growth arrest induced by CXCR4 depletion is cell autonomous and not secondary to effects on the microvasculature.

Pharmacological Inhibition of CXCR4 Arrests MPNST Proliferation and Tumor Growth

We next tested a clinically validated, highly specific CXCR4 antagonist, AMD3100, in our system. We performed a dose-response analysis of AMD3100 on primary murine MPNST cells (SMPNSTs and *cisNP*), one primary human MPNST cell line, three established human MPNST cell lines (S462; SNF02.2; SNF96.2), and pretumor cells (*Nf1;p53* null SKPs) (Figures 6A and 6B). Four of six cell lines were potently inhibited by low doses of AMD3100 (IC_{50} values ≤ 0.5 μ M; Figure 6C). One human MPNST cell line, SNF96.2, and the pretumor cells were less sensitive (IC_{50} values of 1–10 μ M; Figure 6C). Only one human MPNST cell line, SNF02.2, showed no response, which is consistent with its low endogenous CXCR4 levels relative to the other MPNST cells (Figure S6A). Of note, we were unable to seed xenograft tumors using SNF02.2 cells, suggesting that this cell line has drifted significantly from the original tumor of derivation (data not shown). In contrast, the cell viability of wild-type (WT) Schwann cells and SKPs was unaffected by AMD3100 (Figure 6A). Inhibition of CXCR4 by AMD3100 also reduced cyclin D1 levels via the AKT/GSK-3 β / β -catenin pathway (Figure 6D).

To assess the therapeutic potential of AMD3100 in vivo, we first tested subcutaneous allografts of primary SMPNSTs. Trans-

plant recipient animals with palpable tumors were treated with AMD3100 and, after 3 weeks of treatment, were sacrificed for analysis (Figure 6E). AMD3100 treatment potently suppressed MPNST growth, resulting in reduced tumor size and weight that was 38% and 42%, respectively, of the control group (Figure S6B). This was accompanied by commensurate reduction in BrdU incorporation and Ki67 staining (Figures S6C and S6D). Consistent with the in vitro data, AMD3100-treated tumors showed decreased levels of cyclin D1, activated β -catenin, phospho-AKT, and phospho-ser9-GSK-3 β (Figure S6E).

To further validate the role of CXCR4 signaling in MPNST growth and the potent cytostatic effect of AMD3100 on tumor growth, we turned to a spontaneous endogenous GEMM. A mouse strain in which null *p53* and *Nf1* alleles are configured in *cis* on the same chromosome spontaneously develop MPNST via loss of heterozygosity (LOH) of both tumor suppressor alleles (*cisNf/p53*; Vogel et al., 1999). Although a majority of the spontaneous tumors are sarcomas, these *cisNf/p53* mice are also prone to other NF1-initiated tumors such as lymphomas and gliomas, as well as to spontaneous p53-based tumors (Cichowski et al., 1999; Vogel et al., 1999). Based on Kaplan-Meier curve data that indicate spontaneous neurofibrosarcoma appearance with 20% mortality at about 15 weeks of age and 70 percent mortality at 25 weeks (n = 170; Vogel et al., 1999), we commenced the AMD3100 drug trial on *cisNf/p53* mice at 16 weeks of age. As shown in Figure 6F, at 2 months posttreatment (24 weeks of age), 7/10 control mice (70%) had perished, whereas, in the AMD3100 group, only 3/17 (18%) had perished. All perished mice had large tumors, and histopathological analysis of the tumor tissues revealed that one mouse from the control group and one from the experimental group had clear evidence of a primary tumor of hematopoietic origin (Figures S6F and S6G). Therefore, these mice were removed from the study, resulting in a total of nine control mice and 16 AMD3100-treated mice (Figure 6G). Six out of nine control mice developed lethal sarcomas. Five developed MPNST, as evidenced by histopathological analysis and S100 β and GAP43 immunoreactivity (Figure 6F, C1, C2, and C5–C7; Figure S6H). A sixth control mouse died with a malignant triton tumor (MTT), which is an NF1-associated sarcomatous tumor having high myoglobin expression (Figure 6F, C4; and Figure S6I). All six tumors displayed CXCR4 expression (Figure 6F). In contrast to the high mortality rate in the control group, at 2 months posttreatment, only two out of 16 mice from the AMD3100 treatment group had perished with a solid tumor (Figure 6F, AMD1 and AMD3; Figure 6G). By histological analysis, we determined that one of the tumors was a rhabdomyosarcoma (RMS) with very low levels of CXCR4 expression (Figure 6F, AMD3, and Figures S6J and S6K). The second treated mouse developed a leiomyosarcoma (LMS) with CXCR4 expression

(C) Paraffin sections of MPNSTs (harvested from SMPNST-allograft mice injected with either control pLKO-ctrl or CXCR4-depleted pLKO-mCXCR4 SMPNST cells) were stained with antibody against BrdU and counterstained with hematoxylin (blue).

(D) The percentage of SMPNST cells that were BrdU positive was determined for each tumor.

(E and F) Analysis of the expression levels of various cell-cycle genes/proteins in the indicated cells as measured by qPCR (E) and western blotting (F).

(G) Cell growth curves of indicated cells as measured with an ATP luminescence assay.

(H) CXCR4 and cyclin D1 protein levels were examined by western blotting in indicated cells.

Scale bar, 50 μ m. All statistics represent mean \pm SD (*p < 0.05 and **p < 0.01). See also Figure S3.

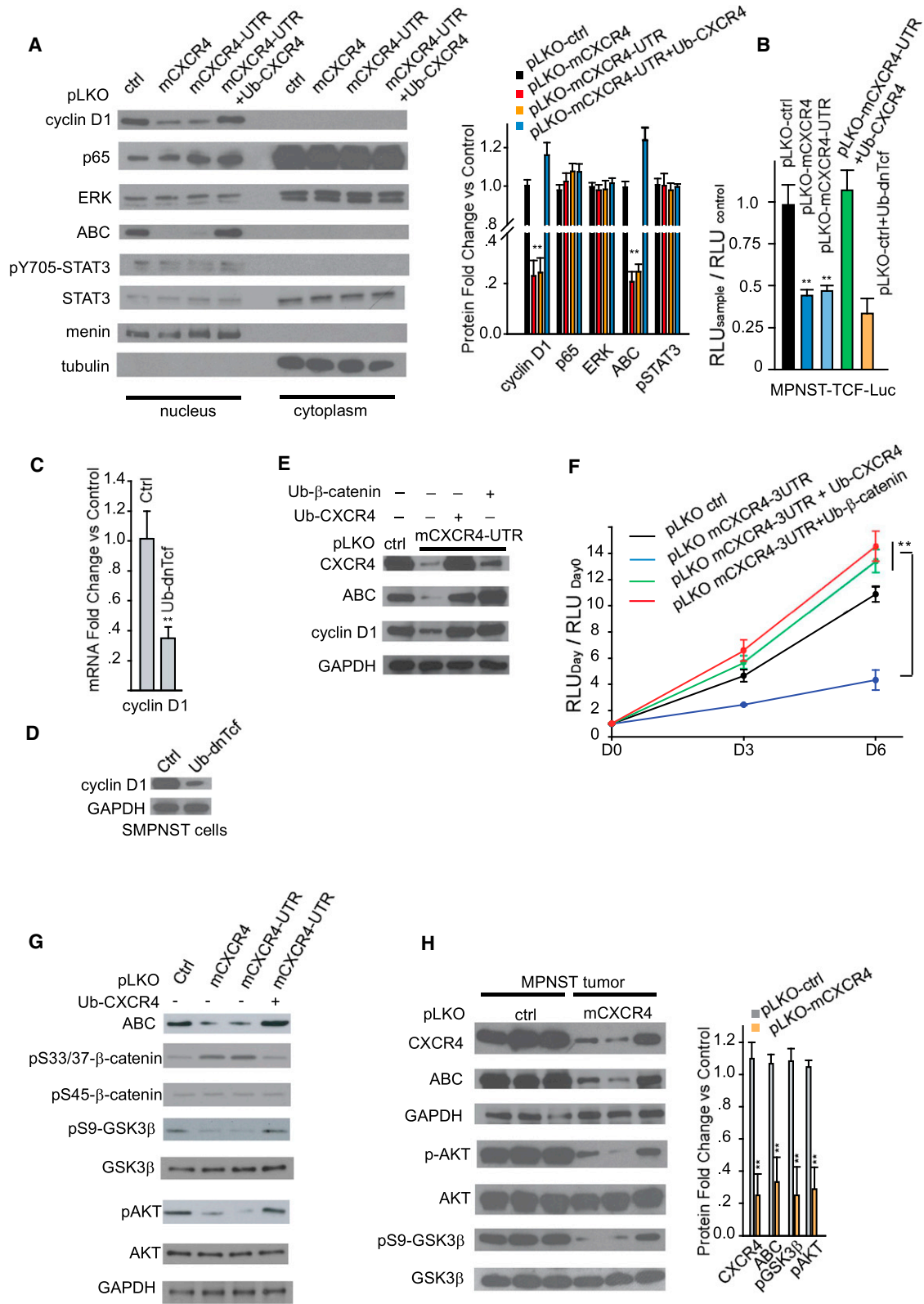


Figure 4. CXCR4 Regulates Cyclin D1 Expression through the AKT/GSK-3β/β-Catenin Network
(A) Immunoblot of nuclear and cytoplasmic extracts from SMPNST cells with indicated antibodies.

(legend continued on next page)

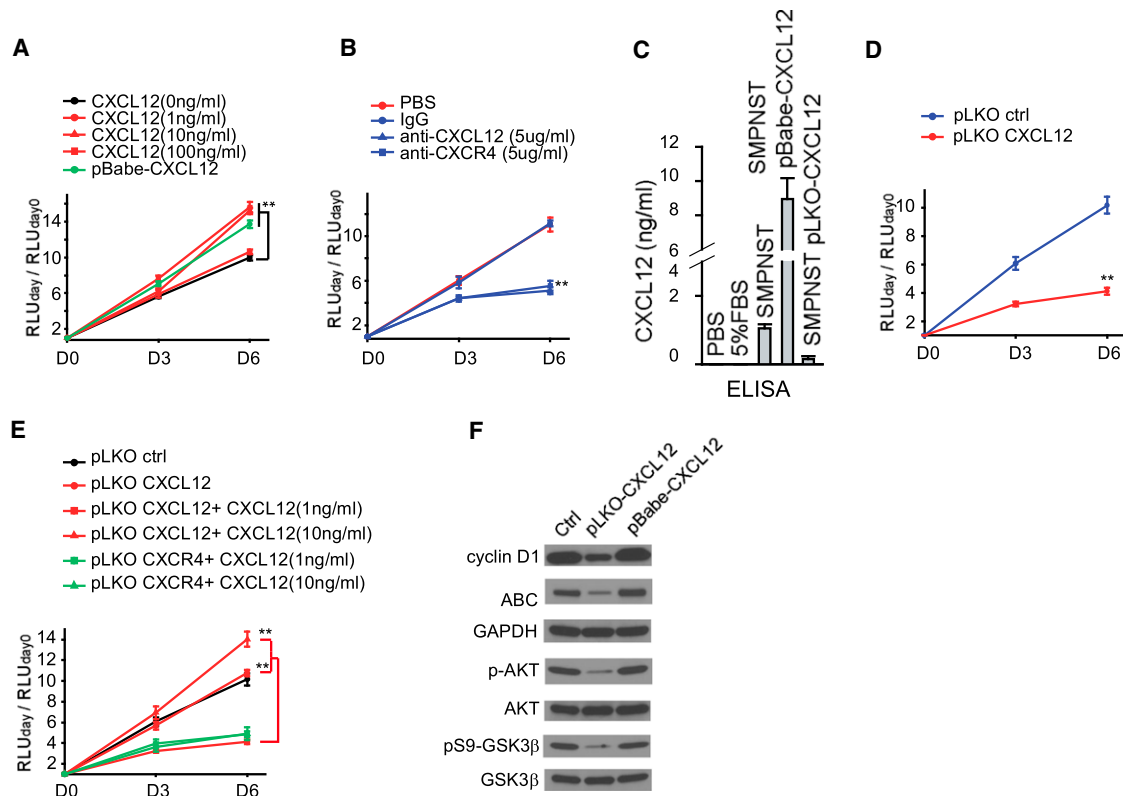


Figure 5. An Autocrine Mechanism Involving CXCL12 and CXCR4 Maintains Growth of MPNST Cells

(A and B) Growth curve of SMPNST cells treated with recombinant CXCL12 protein (A) or CXCL12/CXCR4 antibodies (B).

(C) ELISA to measure CXCL12 protein level in PBS, 5% fetal bovine serum (FBS) Dulbecco's modified Eagle's medium (DMEM) media, and conditioned media from SMPNST cells or SMPNST cells expressing pBabe-CXCL12 (overexpression) or pLKO-CXCL12 (knockdown).

(D) Growth curve of control SMPNST cells (pLKO ctrl) and CXCL12-depleted SMPNST cells (pLKO-CXCL12).

(E) Growth curve of SMPNST cells, CXCR4- or CXCL12-depleted SMPNST cells, and CXCR4- or CXCL12-depleted SMPNST cells treated with recombinant CXCL12 protein.

(F) Immunoblot of cell lysates from SMPNST cells and SMPNST cells expressing pLKO-CXCL12 or pBabe-CXCL12 with indicated antibodies.

All statistics represent mean \pm SD (** $p < 0.01$). See also Figure S5.

(Figure 6F, AMD1, and Figures S6L and S6M), suggesting that this tumor escaped AMD3100 treatment. Whether this outlier reflects failed drug delivery or, alternatively, an independent mechanism of tumor promotion will require additional studies.

In summary, the allograft and genetic tumor model data demonstrate that *in vivo* pharmacological blockade of CXCR4 can potentially inhibit spontaneous MPNST tumor development in a GEMM by blocking the same signaling pathways as observed in primary tumor cultures.

Conserved Signaling Pathway Activation in Human MPNST

The above studies reflect analyses of genetic mouse models extended to a single human tumor and primary MPNST line plus three established human MPNST lines. To further assess the relevance of our findings to human MPNST, we examined CXCR4 in MPNSTs from patients with NF1. We sequenced coding exons 1 and 2 (see [Experimental Procedures](#)) of CXCR4 from a series of NF1-associated human MPNST

(B) Luciferase reporter assay to measure TCF activation in control SMPNST cells (pLKO-ctrl), CXCR4-depleted SMPNST cells (pLKO-mCXCR4 and pLKO-mCXCR4-UTR), CXCR4-depleted SMPNST cells rescued by CXCR4 overexpression (pLKO-mCXCR4-UTR+Ub-CXCR4), and SMPNST cells expressing dominant-negative Tcf (pLKO-ctrl+Ub-dnTcf).

(C and D) The mRNA and protein levels of cyclin D1 in SMPNST cells (ctrl) or SMPNST cells expressing dnTcf (dnTcf) were determined either by qPCR assay (C) or by western blotting (D).

(E) Immunoblot of cell lysates from SMPNST cells, CXCR4-depleted SMPNST cells, and CXCR4-depleted SMPNST cells ectopically expressing CXCR4 or β -catenin with indicated antibodies (ABC: antibody against activated β -catenin).

(F) ATP luminescence assay to measure growth of indicated cells.

(G) Immunoblot of cell lysates from SMPNST cells and CXCR4-depleted SMPNST cells with indicated antibodies.

(H) Graph showing fold change versus control of tumor tissue lysates from control SMPNSTs (ctrl) or SMPNSTs from CXCR4-depleted cells (mCXCR4) with indicated antibodies.

All statistics represent mean \pm SD (** $p < 0.01$). See also Figure S4.

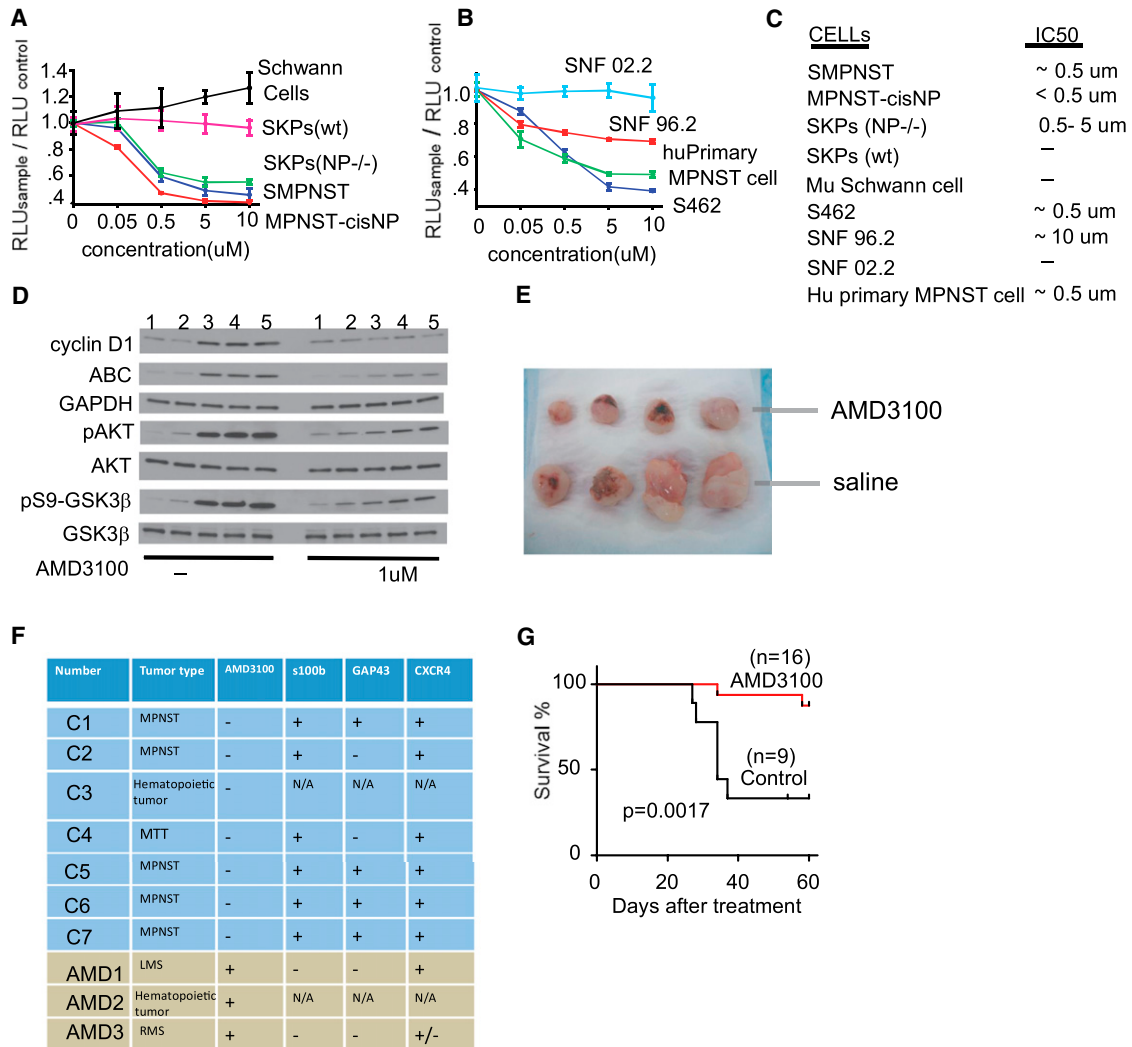


Figure 6. AMD3100 Specifically Inhibits the Proliferation of SMPNST Cells and Suppresses the Growth of MPNSTs In Vivo

(A and B) Dose curve showing effect of AMD3100 on proliferation of murine (primary cells from MPNST SKP model and *cisNP* model) and human (SNF 02.2, SNF 96.2, S462, and primary cells from a human NF1 patient) MPNST cells, pretumor SKP *NP^{-/-}* cells, and WT murine Schwann cells and SKPs.

(C) Experimentally derived AMD3100 IC₅₀ values.

(D) Immunoblot with the indicated antibodies of cell lysates from murine cells in the absence or presence of AMD3100.

(E) Representative picture of the SMPNST-allograft tumors (from nude mice injected with SMPNST cells) during the treatment study with tumor histopathology and immunohistochemistry.

(F) List of control (C-) and AMD3100-treated (AMD-) mice that died during the treatment study, with tumor histopathology and immunohistochemistry.

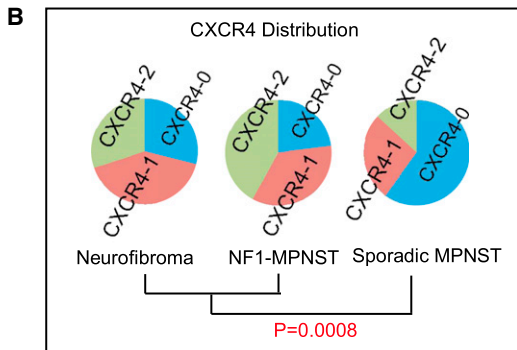
(G) Kaplan-Meier survival curve of mice in the AMD3100 treatment study (control group, n = 9; AMD3100-treated group, n = 16; p = 0.0017 by Mantel-Cox test). Other statistics represent mean ±SD. See also Figure S6.

samples and cell lines (Figure S5A), including S462, which requires CXCR4 function for growth (Figure 6B); all CXCR4 coding regions analyzed had WT sequence (Figure S5A). Thus, similar to the murine MPNSTs, human MPNST CXCR4 activity must depend on ligand presence. We next examined CXCR4 protein expression using a human tissue microarray (TMA) that included 17 plexiform neurofibromas (from NF1 patients harboring MPNSTs) and 73 MPNST samples (43 from NF1 patients and 30 sporadic) (Ghadimi et al., 2012; Zou et al., 2009). The data showed that 94% of neurofibromas and 98% of NF1-deficient MPNSTs displayed CXCR4 immunoreactivity (Figures

7A and 7B), whereas only 66% of sporadic MPNSTs tissues showed CXCR4 immunoreactivity. Similarly, 71% of neurofibromas and 77% of NF1-associated MPNSTs exhibited CXCR4 expression in >5% of tumor cells, as compared to 40% of sporadic MPNST tissues (Figure 7A). Spearman correlation analysis showed a statistically significant difference in CXCR4 intensity and distribution when comparing NF1-associated tumors to sporadic tumors (two-sided p = 0.0012 and 0.0008, respectively) (Figure 7B). We also assessed p-AKT, β-catenin, and cyclin D1 expression and observed a direct concordance between their levels and those of CXCR4 (p = 0.0198,

A

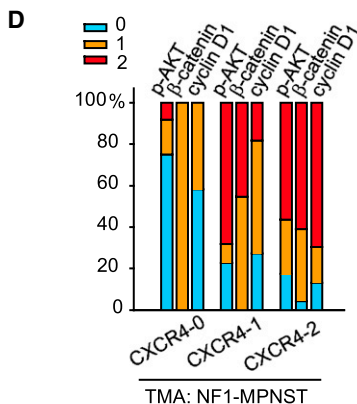
	CXCR4 Intensity			CXCR4 Distribution		
	0	1	2	0	1	2
Neurofibroma (n=17)	1 (6%)	9 (53%)	7 (41%)	5 (29%)	7 (41%)	5 (30%)
NF1-MPNST (n=43)	1 (2%)	33 (77%)	9 (21%)	10 (23%)	15 (35%)	18 (42%)
Sporadic MPNST (n=30)	10 (33%)	16 (53%)	4 (13%)	18 (60%)	8 (27%)	4 (13%)



C

	CXCR4 %	p-AKT %	β -cat Intensity	Cyclin D1 %
Correlation coefficient	1	0.362902554	0.447397261	0.556450893
valid cases	43	41	42	40
one-sided significance	0	0.009851018	0.001485603	9.62895E-05

* p-value by 2 for two-sided



0.0028, and 1.93×10^{-4} , respectively) (Figures 7C and 7D). Thus, TMA data confirm that AKT/GSK-3 β // β -catenin pathway activation is conserved in human NF1-associated MPNSTs. Extension of our functional data in murine and human MPNST cells, coupled with the TMA studies, indicate that CXCR4 and cyclin D1 are closely associated with clinical NF1-associated pathogenesis.

DISCUSSION

We exploited the unique properties of GEMMs for NF1-associated MPNST that permitted isolation and direct comparison with tumor cells of origin and precursor nontumor cells. The progressively elevated expression of the chemokine receptor CXCR4 along the increasingly tumorigenic series from prealign-

Figure 7. Analysis of CXCR4 Expression and Downstream Pathway Signaling Reveals Conservation in Human MPNSTs

(A) Quantification of the intensity and distribution of CXCR4 immunoreactive cells in all MPNST TMAs.

(B) Schema of the CXCR4 distribution in TMAs. Spearman correlation identified a statistically significant difference between NF1-associated and sporadic tumors ($p = 0.0008$).

(C) Spearman correlation coefficient analyses between CXCR4, pAKT, β -catenin, and cyclin D1 in NF1-MPNST.

(D) Quantification of pAKT, β -catenin, and cyclin D1 expression levels in MPNST-NF1 TMA and categorization based on CXCR4 expression level. Staining distribution of positively staining cells: (0) = <5%, (1) = 5%–30%, (2) >30%, and intensity: (0) = negative, (1) = low, and (2) = intermediate to high. Spearman's correlation coefficient analyses were used to determine the concordance between CXCR4 expression and NF1 status and between CXCR4 and other biomarkers.

nant *Nf1* null and *Nf/p53* double null tumor progenitors to *Nf1* null benign tumors (neurofibromas) and, finally, to *Nf/p53* double null MPNSTs drew our attention and motivated the present study.

CXCR4/CXCL12: An MPNST Autocrine Loop

We also found increased CXCR4 expression in human NF1 patient tumor samples and primary cells. CXCR4 is commonly found in human and experimental murine cancers. Protumorigenic paracrine functions attributed to this G-protein-coupled receptor/ligand include cell homing, migration, and induction of neovascularization (Li et al., 2004; Sengupta et al., 2012; Singh et al., 2004). In the present study, we identify an autocrine loop in

cells that sustains activated CXCR4. MPNST cells with CXCR4 depletion exhibit proliferative arrest rather than cell death, with fewer cells in S phase. Consistent with this, we found that the G1/S phase transition protein cyclin D1 responded to altered CXCR4 expression.

CXCR4 signaling differs in normal and cancer cells both at the functional and molecular signaling levels. For example, CXCL12 treatment of WT primary neonatal astrocytes induced apoptosis, whereas it promoted enhanced survival in astrocytoma cultures (Warrington et al., 2007). In our study, CXCR4 suppression inhibited MPNST cell progression from G1 to S phase in the cell cycle and resulted in potent inhibition of MPNST cell growth in vitro and also in vivo tumor growth in several experimental paradigms. MPNST cells with either chronic or acute CXCR4 knockdown were deficient in allograft transplantations.

Administration of the CXCR4 inhibitor, AMD3100, also impeded efficient tumor allotransplantation of murine MPNSTs. In perhaps the most stringent assay, spontaneous MPNST development was dramatically inhibited in a *cisNf/p53* GEMM. This result illustrates the potential power of spontaneous genetically relevant malignant tumor mouse models as experimental tools for cancer treatment discovery.

Our data point to a cell-autonomous pathway of activation but do not rule out potential ligand contribution from other tumor-associated sources. However, MPNST cells themselves provide sufficient ligand to sustain autocrine cell growth in culture. We make note that, although our CXCR4 shRNA experiments provide similar allograft growth inhibition to that of AMD3100, our studies do not address the possibility that pharmacological inhibition of CXCR4 may extend to additional targets such as bone-marrow-derived cells that may result in additional tumor inhibitory effects.

CXCR4 Promotes MPNST Proliferation via PI3K and GSK-3 β

The function of the NF1 protein neurofibromin as a RAS-GTPase-activating protein has traditionally focused attention on the two main Ras effector pathways: raf/erk and PI3K/mTOR. Inhibition of the erk pathway can impact and even lead to reversal of certain NF1 mutation-based phenotypes (Cui et al., 2008; Wang et al., 2012). Other studies have reported that hyperactivation of the mTOR pathway underlies a growth advantage in NF1-deficient MPNST cells and that rapamycin-mediated inhibition of mTOR blunts MPNST growth in vivo (Johannessen et al., 2008; Johansson et al., 2008). We saw modest downmodulation of p-mTOR but saw no effects on p-S6 signaling in our SMPNST system. In our study, NF1 loss specifically caused upregulation of Akt/PI3Kinase, but not of Erk. By recent accounting, more than 25 positive and negative effectors of Akt signaling have been described (<http://www.proteinLounge.com>). How specific pathways are selected for activity in a given cellular context may depend in part on the AKT isoform, intracellular localization of the active intermediates, and other factors not yet understood.

The association of CXCR4 with various cancers has implicated activation of several signaling effectors, including PLC γ /Ca²⁺, PI3K/AKT/NF κ B, and Erk/p38, leading to chemotaxis, survival, angiogenesis, etc. (Balkwill, 2004). In MPNSTs, however, CXCR4 depletion deactivated AKT, but not ERK or PLC γ , thus revealing cell context-specific pathway regulation. mTORC1 and GSK-3 β are important downstream effectors of phospho-AKT, and our results show that, in MPNSTs, CXCR4 depletion more strongly impacts GSK-3 β rather than mTOR through PI3K and that GSK-3 β mediates cyclin D1 expression. Thus, we propose that the PI3K/GSK-3 β branch downstream of CXCR4 is sufficient to promote MPNST proliferation. These studies, however, do not rule out that additional signaling pathways and effectors of AKT, β -catenin, and TCF may have contributory functions in MPNST progression.

Soft tissue sarcomas are among the most therapy-resistant and life-threatening forms of cancer. Our data indicate that correction of abnormal CXCR4 signaling may be a promising therapeutic target for NF1-associated MPNSTs. In addition, a subset of sporadic MPNSTs may also co-opt this signaling

mechanism, in which case CXCR4 attenuation could potentially benefit this patient population. Clinically-relevant CXCR4 inhibitors were initially developed for the treatment of HIV (Peled et al., 2012). These include compounds of four different classes: small-molecule inhibitors (e.g., AMD3100), small modified peptides (e.g., BTK140), antibodies (e.g., ALX-0651), and modified CXCL12 antagonists (e.g., CTCE-9908). Given the accumulating evidence for the important role of this paracrine axis in cancer, such compounds are currently being tested in early-phase clinical trials (<http://www.clinicaltrials.gov>). Our preclinical observations supplemented by strong evidence that the CXCR4 axis activity is sustained in human samples support the inclusion of MPNST patients in such studies. Notably, effects of CXCR4 blockade are cytostatic rather than cytotoxic. However, taking into account that surgery is the mainstay of MPNST treatment, therapeutic approaches such as CXCR4 inhibition may improve local growth control and enhance resectability. In addition, sustained blockade of tumor development may provide an opportunity for endogenous inflammatory and immune anti-tumor responses to gain a foothold. Moreover, the identification of additional pathways that can be targeted in combination with CXCR4 will hopefully result in synthetic lethality and superior anti-MPNST effects. Further studies will resolve this important question.

EXPERIMENTAL PROCEDURES

All experimental procedures are described in detail in the [Extended Experimental Procedures](#).

MPNST Mouse Models

SKP MPNST Model

SKPs were isolated as previously reported (Le et al., 2009) from *Nf1/f; p53/f; Rosa26-LacZ* mice. 10⁵ NP^{-/-} SKPs were implanted subcutaneously into the same mouse from which the SKPs were originally isolated (SMPNST autograft). The autologously transplanted SKPs gave rise to MPNSTs within 2 months after implantation 100% of the time. The tumors exhibited all the characteristics of human MPNST, including fascicular patterns of tightly packed spindle cells with hyperchromatic nuclei and frequent mitoses, as well as S100B expression (L.Q.L., T. Shipman, and L.F.P., unpublished data).

SMPNST Allograft Model

SMPNST cells were subcutaneously injected into the backs of 5- to 6-week-old athymic nude mice.

*cis*NP MPNST Model

A spontaneous endogenous GEMM for MPNSTs. We utilized a mouse strain in which null *p53* and *Nf1* alleles are configured in *cis* on the same chromosome and spontaneously develop MPNST via loss of heterozygosity of both tumor suppressor alleles (Vogel et al., 1999).

AMD3100 and Doxycycline Treatment In Vivo; Measurement of Tumor Volume

AMD3100 Treatment of MPNST Allograft Model

MPNST cells were subcutaneously injected into the backs of 5- to 6-week-old female athymic nude mice. The CXCR4 inhibitor AMD3100 was administered subcutaneously daily at 5 mg/kg of body weight, beginning at the time of tumor detection.

AMD3100 Treatment of GEMM

AMD3100 (130 μ g/d) or saline was administered using subcutaneously implanted osmotic minipumps (DURECT Corporation). Two month treatment began when the mice were 16 weeks old.

Doxycycline was delivered in 5% sucrose-containing drinking water at 1 mg/ml. Tumor size was calculated by measuring length and width of the

lesion with the formula (length) \times (width)² \times (0.52). All statistical analyses were done with Student's *t* test.

SUPPLEMENTAL INFORMATION

Supplemental Information includes Extended Experimental Procedures and six figures and can be found with this article online at <http://dx.doi.org/10.1016/j.cell.2013.01.053>.

ACKNOWLEDGMENTS

We thank Karen Cichowski for the generous gift of the human MPNST cell lines. This work was partially supported by funding from the National Cancer Institute (grant R01 CA166593 to L.Q.L.), Department of Defense (grant W81XWH-12-1-0161 to L.Q.L. and Postdoctoral Fellowship Award grant W81XWH-11-1-0184 to W.M.), and the National Institutes of Health (grant P50NS052606 to L.F.P.). L.Q.L. is a Disease-Oriented Clinical Scholar and holds a Career Award for Medical Scientists from the Burroughs Wellcome Fund. L.F.P. is an American Cancer Society Research Professor.

Received: June 8, 2012

Revised: November 21, 2012

Accepted: January 30, 2013

Published: February 21, 2013

REFERENCES

- Balkwill, F. (2004). The significance of cancer cell expression of the chemokine receptor CXCR4. *Semin. Cancer Biol.* *14*, 171–179.
- Bertolini, F., Dell'Agnola, C., Mancuso, P., Rabascio, C., Burlini, A., Monestirli, S., Gobbi, A., Pruneri, G., and Martinelli, G. (2002). CXCR4 neutralization, a novel therapeutic approach for non-Hodgkin's lymphoma. *Cancer Res.* *62*, 3106–3112.
- Bian, X.W., Yang, S.X., Chen, J.H., Ping, Y.F., Zhou, X.D., Wang, Q.L., Jiang, X.F., Gong, W., Xiao, H.L., Du, L.L., et al. (2007). Preferential expression of chemokine receptor CXCR4 by highly malignant human gliomas and its association with poor patient survival. *Neurosurgery* *61*, 570–578, discussion 578–579.
- Burger, J.A., Burger, M., and Kipps, T.J. (1999). Chronic lymphocytic leukemia B cells express functional CXCR4 chemokine receptors that mediate spontaneous migration beneath bone marrow stromal cells. *Blood* *94*, 3658–3667.
- Cichowski, K., Shih, T.S., Schmitt, E., Santiago, S., Reilly, K., McLaughlin, M.E., Bronson, R.T., and Jacks, T. (1999). Mouse models of tumor development in neurofibromatosis type 1. *Science* *286*, 2172–2176.
- Cross, D.A., Alessi, D.R., Cohen, P., Andjelkovich, M., and Hemmings, B.A. (1995). Inhibition of glycogen synthase kinase-3 by insulin mediated by protein kinase B. *Nature* *378*, 785–789.
- Cui, Y., Costa, R.M., Murphy, G.G., Elgersma, Y., Zhu, Y., Gutmann, D.H., Parada, L.F., Mody, I., and Silva, A.J. (2008). Neurofibromin regulation of ERK signaling modulates GABA release and learning. *Cell* *135*, 549–560.
- Ferner, R.E. (2007). Neurofibromatosis 1. *Eur. J. Hum. Genet.* *15*, 131–138.
- Ghadimi, M.P., Young, E.D., Belousov, R., Zhang, Y., Lopez, G., Lusby, K., Kivlin, C., Demicco, E.G., Creighton, C.J., Lazar, A.J., et al. (2012). Survivin is a viable target for the treatment of malignant peripheral nerve sheath tumors. *Clin. Cancer Res.* *18*, 2545–2557.
- Hoppler, S., and Kavanagh, C.L. (2007). Wnt signalling: variety at the core. *J. Cell Sci.* *120*, 385–393.
- Johannessen, C.M., Johnson, B.W., Williams, S.M., Chan, A.W., Reczek, E.E., Lynch, R.C., Rieth, M.J., McClatchey, A., Ryeom, S., and Cichowski, K. (2008). TORC1 is essential for NF1-associated malignancies. *Curr. Biol.* *18*, 56–62.
- Johansson, G., Mahler, Y.Y., Collins, M.H., Kim, M.O., Nobukuni, T., Perentesis, J., Cripe, T.P., Lane, H.A., Kozma, S.C., Thomas, G., and Ratner, N. (2008). Effective in vivo targeting of the mammalian target of rapamycin pathway in malignant peripheral nerve sheath tumors. *Mol. Cancer Ther.* *7*, 1237–1245.
- Johnson, D.G., and Walker, C.L. (1999). Cyclins and cell cycle checkpoints. *Annu. Rev. Pharmacol. Toxicol.* *39*, 295–312.
- Joseph, N.M., Mosher, J.T., Buchstaller, J., Snider, P., McKeever, P.E., Lim, M., Conway, S.J., Parada, L.F., Zhu, Y., and Morrison, S.J. (2008). The loss of Nf1 transiently promotes self-renewal but not tumorigenesis by neural crest stem cells. *Cancer Cell* *13*, 129–140.
- Kijima, T., Maulik, G., Ma, P.C., Tibaldi, E.V., Turner, R.E., Rollins, B., Sattler, M., Johnson, B.E., and Salgia, R. (2002). Regulation of cellular proliferation, cytoskeletal function, and signal transduction through CXCR4 and c-Kit in small cell lung cancer cells. *Cancer Res.* *62*, 6304–6311.
- Koshiba, T., Hosotani, R., Miyamoto, Y., Ida, J., Tsuji, S., Nakajima, S., Kawaguchi, M., Kobayashi, H., Doi, R., Hori, T., et al. (2000). Expression of stromal cell-derived factor 1 and CXCR4 ligand receptor system in pancreatic cancer: a possible role for tumor progression. *Clin. Cancer Res.* *6*, 3530–3535.
- Laverdiere, C., Hoang, B.H., Yang, R., Sowers, R., Qin, J., Meyers, P.A., Huvos, A.G., Healey, J.H., and Gorlick, R. (2005). Messenger RNA expression levels of CXCR4 correlate with metastatic behavior and outcome in patients with osteosarcoma. *Clin. Cancer Res.* *11*, 2561–2567.
- Le, L.Q., and Parada, L.F. (2007). Tumor microenvironment and neurofibromatosis type 1: connecting the GAPs. *Oncogene* *26*, 4609–4616.
- Le, L.Q., Shipman, T., Burns, D.K., and Parada, L.F. (2009). Cell of origin and microenvironment contribution for NF1-associated dermal neurofibromas. *Cell Stem Cell* *4*, 453–463.
- Le, L.Q., Liu, C., Shipman, T., Chen, Z., Suter, U., and Parada, L.F. (2011). Susceptible stages in Schwann cells for NF1-associated plexiform neurofibroma development. *Cancer Res.* *71*, 4686–4695.
- Lee, M.H., and Yang, H.Y. (2003). Regulators of G1 cyclin-dependent kinases and cancers. *Cancer Metastasis Rev.* *22*, 435–449.
- Li, Y.M., Pan, Y., Wei, Y., Cheng, X., Zhou, B.P., Tan, M., Zhou, X., Xia, W., Horstobagyi, G.N., Yu, D., and Hung, M.C. (2004). Upregulation of CXCR4 is essential for HER2-mediated tumor metastasis. *Cancer Cell* *6*, 459–469.
- Liu, C., Li, Y., Semenov, M., Han, C., Baeg, G.H., Tan, Y., Zhang, Z., Lin, X., and He, X. (2002). Control of beta-catenin phosphorylation/degradation by a dual-kinase mechanism. *Cell* *108*, 837–847.
- Mantripragada, K.K., Spurlock, G., Kluwe, L., Chuzhanova, N., Ferner, R.E., Frayling, I.M., Dumanski, J.P., Guha, A., Mautner, V., and Upadhyaya, M. (2008). High-resolution DNA copy number profiling of malignant peripheral nerve sheath tumors using targeted microarray-based comparative genomic hybridization. *Clin. Cancer Res.* *14*, 1015–1024.
- Müller, A., Homey, B., Soto, H., Ge, N., Catron, D., Buchanan, M.E., McClanahan, T., Murphy, E., Yuan, W., Wagner, S.N., et al. (2001). Involvement of chemokine receptors in breast cancer metastasis. *Nature* *410*, 50–56.
- Obaya, A.J., and Sedivy, J.M. (2002). Regulation of cyclin-Cdk activity in mammalian cells. *Cell. Mol. Life Sci.* *59*, 126–142.
- Oh, J.W., Drabik, K., Kutsch, O., Choi, C., Tousson, A., and Benveniste, E.N. (2001). CXCR4 chemokine receptor 4 expression and function in human astrogloma cells. *J. Immunol.* *166*, 2695–2704.
- Peled, A., Wald, O., and Burger, J. (2012). Development of novel CXCR4-based therapeutics. *Expert Opin. Investig. Drugs* *21*, 341–353.
- Righi, E., Kashiwagi, S., Yuan, J., Santosuosso, M., Leblanc, P., Ingraham, R., Forbes, B., Edelblute, B., Collette, B., Xing, D., et al. (2011). CXCL12/CXCR4 blockade induces multimodal antitumor effects that prolong survival in an immunocompetent mouse model of ovarian cancer. *Cancer Res.* *71*, 5522–5534.
- Rubin, J.B., and Gutmann, D.H. (2005). Neurofibromatosis type 1 - a model for nervous system tumour formation? *Nat. Rev. Cancer* *5*, 557–564.
- Schrader, A.J., Lechner, O., Templin, M., Dittmar, K.E., Machtens, S., Mengel, M., Probst-Kepper, M., Franzke, A., Wollensak, T., Gatzlaff, P., et al. (2002). CXCR4/CXCL12 expression and signalling in kidney cancer. *Br. J. Cancer* *86*, 1250–1256.

- Sehgal, A., Keener, C., Boynton, A.L., Warrick, J., and Murphy, G.P. (1998). CXCR-4, a chemokine receptor, is overexpressed in and required for proliferation of glioblastoma tumor cells. *J. Surg. Oncol.* *69*, 99–104.
- Sengupta, R., Dubuc, A., Ward, S., Yang, L., Northcott, P., Woerner, B.M., Kroll, K., Luo, J., Taylor, M.D., Wechsler-Reya, R.J., and Rubin, J.B. (2012). CXCR4 activation defines a new subgroup of Sonic hedgehog-driven medulloblastoma. *Cancer Res.* *72*, 122–132.
- Serra, E., Rosenbaum, T., Winner, U., Aledo, R., Ars, E., Estivill, X., Lenard, H.G., and Lázaro, C. (2000). Schwann cells harbor the somatic NF1 mutation in neurofibromas: evidence of two different Schwann cell subpopulations. *Hum. Mol. Genet.* *9*, 3055–3064.
- Sherr, C.J. (1995). D-type cyclins. *Trends Biochem. Sci.* *20*, 187–190.
- Singh, S., Singh, U.P., Grizzle, W.E., and Lillard, J.W., Jr. (2004). CXCL12-CXCR4 interactions modulate prostate cancer cell migration, metalloproteinase expression and invasion. *Lab. Invest.* *84*, 1666–1676.
- Srivastava, A.K., and Pandey, S.K. (1998). Potential mechanism(s) involved in the regulation of glycogen synthesis by insulin. *Mol. Cell. Biochem.* *182*, 135–141.
- Taichman, R.S., Cooper, C., Keller, E.T., Pienta, K.J., Taichman, N.S., and McCauley, L.K. (2002). Use of the stromal cell-derived factor-1/CXCR4 pathway in prostate cancer metastasis to bone. *Cancer Res.* *62*, 1832–1837.
- Tongsgard, J.H. (2006). Clinical manifestations and management of neurofibromatosis type 1. *Semin. Pediatr. Neurol.* *13*, 2–7.
- Vogel, K.S., Klesse, L.J., Velasco-Miguel, S., Meyers, K., Rushing, E.J., and Parada, L.F. (1999). Mouse tumor model for neurofibromatosis type 1. *Science* *286*, 2176–2179.
- Wang, Z., Ma, Q., Liu, Q., Yu, H., Zhao, L., Shen, S., and Yao, J. (2008). Blockade of SDF-1/CXCR4 signalling inhibits pancreatic cancer progression in vitro via inactivation of canonical Wnt pathway. *Br. J. Cancer* *99*, 1695–1703.
- Wang, Y., Kim, E., Wang, X., Novitch, B.G., Yoshikawa, K., Chang, L.S., and Zhu, Y. (2012). ERK inhibition rescues defects in fate specification of Nf1-deficient neural progenitors and brain abnormalities. *Cell* *150*, 816–830.
- Warrington, N.M., Woerner, B.M., Dagainakatte, G.C., Dasgupta, B., Perry, A., Gutmann, D.H., and Rubin, J.B. (2007). Spatiotemporal differences in CXCL12 expression and cyclic AMP underlie the unique pattern of optic glioma growth in neurofibromatosis type 1. *Cancer Res.* *67*, 8588–8595.
- Zeelenberg, I.S., Ruuls-Van Stalle, L., and Roos, E. (2003). The chemokine receptor CXCR4 is required for outgrowth of colon carcinoma micrometastases. *Cancer Res.* *63*, 3833–3839.
- Zheng, H., Chang, L., Patel, N., Yang, J., Lowe, L., Burns, D.K., and Zhu, Y. (2008). Induction of abnormal proliferation by nonmyelinating schwann cells triggers neurofibroma formation. *Cancer Cell* *13*, 117–128.
- Zhou, Y., Larsen, P.H., Hao, C., and Yong, V.W. (2002). CXCR4 is a major chemokine receptor on glioma cells and mediates their survival. *J. Biol. Chem.* *277*, 49481–49487.
- Zhu, Y., and Parada, L.F. (2001). Neurofibromin, a tumor suppressor in the nervous system. *Exp. Cell Res.* *264*, 19–28.
- Zhu, Y., Ghosh, P., Charnay, P., Burns, D.K., and Parada, L.F. (2002). Neurofibromas in NF1: Schwann cell origin and role of tumor environment. *Science* *296*, 920–922.
- Zou, C.Y., Smith, K.D., Zhu, Q.S., Liu, J., McCutcheon, I.E., Slopis, J.M., Meric-Bernstam, F., Peng, Z., Bornmann, W.G., Mills, G.B., et al. (2009). Dual targeting of AKT and mammalian target of rapamycin: a potential therapeutic approach for malignant peripheral nerve sheath tumor. *Mol. Cancer Ther.* *8*, 1157–1168.